Heliyon 10 (2024) e32850

Contents lists available at ScienceDirect

Heliyon

journal homepage: www.cell.com/heliyon

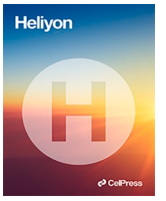

Research article

Modified five times simulated body fluid for efficient biomimetic mineralization

Kun Fu [a,*], Lei-Lei Yang [a], Ning Gao [a], Pengbi Liu [b], Bo Xue [b], Wei He [a], Weiliu Qiu [c], Xuejun Wen [b]

[a] Department of Stomatology, the First Affiliated Hospital of Zhengzhou University, Zhengzhou, Henan, 450052, China
[b] Department of Chemical and Life Science Engineering, School of Engineering, Virginia Commonwealth University, Richmond, VA, 23284, USA
[c] Department of Oral & Maxillofacial Surgery, Ninth People's Hospital, Shanghai Jiao Tong University, Shanghai, 200011, China

ARTICLE INFO

Keywords:
Bone tissue engineering
Biomineralization
Simulated body fluid
Aligned nanofibers

ABSTRACT

Simulated body fluid (SBF) is widely utilized in preclinical research for estimating the mineralization efficacy of biomaterials. Therefore, it is of great significance to construct an efficient and stable SBF mineralization system. The conventional SBF solutions cannot maintain a stable pH value and are prone to precipitate homogeneous calcium salts at the early stages of the biomimetic process because of the release of gaseous CO_2. In this study, a simple but efficient five times SBF buffered by 5 % CO_2 was developed and demonstrated to achieve excellent mineralized microstructure on a type of polymer-aligned nanofibrous scaffolds, which is strikingly similar to the natural human bone tissue. Scanning electron microscopy and energy-dispersive X-ray examinations indicated the growth of heterogeneous apatite with a high-calcium-to-phosphate ratio on the aligned nanofibers under 5 times SBF buffered by 5 % CO_2. Moreover, X-ray diffraction spectroscopy and Fourier transform infrared analyses yielded peaks associated with carbonated hydroxyapatite with less prominent crystallization. In addition, the biomineralized aligned polycaprolactone nanofibers demonstrated excellent cell attachment, alignment, and proliferation characteristics in vitro. Overall, the results of this study showed that 5 × SBFs buffered by 5 % CO_2 partial pressure are attractive alternatives for the efficient biomineralization of scaffolds in bone tissue engineering, and could be used as a model for the prediction of the bone-bonding bioactivity of biomaterials.

1. Introduction

Bone tissue engineering is expected to be an effective strategy for the clinical treatment of patients with bone defects [1,2]. Various biologically active scaffolds were developed as carriers to induce stem cell proliferation and osteogenesis-oriented differentiation, thereby promoting bone regeneration [1–4]. Oriented fibers can guide the directional adhesion and colonization of mesenchymal stem cells, while the loose fiber structure facilitates nutrient and metabolite exchange [5]. Polycaprolactone (PCL), a biodegradable medical polymer certified by the US Food and Drug Administration, exhibits excellent biocompatibility [6,7]. Moreover, PCL possesses a relatively slow degradation rate, making it an ideal polymer for constructing nanofiber scaffolds in bone regeneration research [6,8]. However, PCL nanofiber scaffolds have drawbacks such as low mechanical strength and inadequate hydrophilicity [6], rendering them

* Corresponding author.
E-mail addresses: fkkq01@126.com (K. Fu), heweizdyfy@163.com (W. He), qiuwl@cae.cn (W. Qiu), xwen@vcu.edu.cn (X. Wen).

https://doi.org/10.1016/j.heliyon.2024.e32850
Received 16 January 2024; Received in revised form 9 June 2024; Accepted 11 June 2024
Available online 12 June 2024

unsuitable for the direct construction of osteogenic microenvironments. Incorporating hydroxyapatite into nanofiber scaffold composites enhances both fiber mechanical strength and scaffold osteogenesis guiding ability. Simulated body fluid (SBF), which simulates the inorganic composition of human plasma, is commonly employed to form calcium phosphate coatings on fiber surfaces due to its simplicity, mild reaction conditions, low cost, and resulting apatite structure and composition that closely resemble bone tissue [9–11]. However, the traditional SBF solution has long been questioned to possess the osteogenic potential of biomaterials [10].

The process of SBF immersion is simple under mild reaction conditions, and the chemical composition of the formed apatite is closer to that of natural bone [12]. However, biomineralization in classical SBF is slow and requires fresh solution [10,13]. High-supersaturated SBFs (such as 5 × SBF) can considerably accelerate the process of biomimetic mineralization, but the solutions cannot maintain a stable pH value and are prone to precipitate homogeneous calcium salts at the early stages of the biomimetic process because of the escape of gaseous CO_2 [14–19]. Therefore, a set of stable and efficient SBF systems is urgently required for investigating the potential of existing and newly developed bio-mineral materials. In this study, a simple but efficient modified 5 × SBF solution that was pumped with 5 % CO_2 was developed, which was demonstrated to maintain the constant pH value for a long time. More importantly, taking advantage of a type of aligned PCL nanofibrous scaffolds [20], the modified SBF systems were revealed to induce mineralized crystallization with excellent morphology that resembles the bone tissue. Compared with traditional SBF solution, the mineralized crystallization under modified SBF solution showed a higher calcium-phosphorus and calcium-magnesium ratio. Additionally, we also observed that a higher oscillation speed of 200 rpm yielded superior surface mineralization of PCL fibers in modified SBF solutions. Furthermore, the mineralized crystallization under modified SBF solution showed good biocompatibility to support the proliferation and osteogenic differentiation of human embryonic palatal mesenchymal. Therefore, this modified SBF solution could serve as an important tool for predicting the osteogenic potential of various biomaterials. This type of modified SBF solution can also be used for the surface modification of three-dimensional mesoporous materials.

2. Experimental section

2.1. Fabrication of nanofibrous scaffold

The aligned nanofibers were prepared with the use of electrospinning and a parallel dynamic collection device [5]. PCL (17 g, Mn 80,000, Sigma, St. Louis, Missouri, United States was dissolved in 100 ml Dimethylformamide (DMF) and Dichloromethane (DCM) (v: v = 1:3) to prepare a 17 % (w/v) electrospinning solution. The PCL solution was pumped into a 3 ml syringe fitted with a 21G blunt needle at the feed rate of 0.025 ml min^{-1}. The needle tip was held 10 cm above the collection tracks, and a voltage of 10 kV was applied. The tracks of the parallel dynamic collection device ran at speeds of 50 mm s^{-1}, and the nanofibers were collected at the bottom of the rotating tracks for 7 min. The fibers were then bonded to a 25 mm stainless steel ring by silica gel to prepare the nanofibrous scaffolds and were dried in a vacuum to remove the residual organic solvents during electrospinning.

2.2. Preparation of 5 × SBF

The 5 × SBF was prepared according to the previous study [21]. In brief, 40.62 g NaCl, 1.86 g KCl, 1.84 g $CaCl_2.2H_2O$, 1.52 g $MgCl_2.6H_2O$, 0.6 g Na_2HPO_4, and 0.36 g Na_2SO_4 were fully dissolved in 900 ml of deionized (DI) water. During the process, the solution was evenly heated up to 36.5 ± 0.5 °C and the pH value of the solution was raised by dissolving $NaHCO_3$ and modified with 1 mol/L HCl. The total amount of solution was added up to 1000 ml using DI water, and the final pH value of 5 × SBF was 6.4 ± 0.05.

2.3. Biomineralization process

The surface hydrolysis of fibers was conducted by immersion in a 0.1 N NaOH solution for 45 min before the biomineralization process. After hydrolysis with 0.1 N NaOH, the surface of PCL fibers is enriched with hydroxyl and carboxyl functional groups [22]. Subsequently, the functional groups of PCL capture Ca^{2+} ions from HBF, facilitating the attraction of PO_4^{3-} ions and resulting in the formation of multiple point-like distributed crystal nuclei. The samples were then rinsed with DI water and immersed vertically in 80 ml 5 × SBF on an oscillator in a cell incubator in the presence of 5 % CO_2 at 37 °C (modified 5 × SBF, simulated human blood environment, referred to as C_5) or without CO_2 (traditional 5 × SBF, simulated atmospheric environment, referred to as C_0). The fiber scaffolds were incubated for 12, 24, and 36 h at the oscillation speeds of 0, 150, or 200 revolutions per minute (rpm). After immersion in 5 × SBF SBF for a set time, the specimens were removed, washed with DI water three times, and then dried in a vacuum hood for further characterization.

2.4. Stability and pH change of 5 × SBF

The simulated body fluid properties were observed, and the pH values of the solution at different oscillation speeds were measured at the set time. Specifically, the tests were conducted at 2, 4, 6, 8, 10, 12, 24, and 36 h after the beginning of biomineralization at an oscillation speed of 200 rpm. Each experimental group comprised three samples. Before measuring the pH, the standard solution was calibrated at room temperature.

2.5. Weight change

All PCL scaffolds were accurately weighed before (w1) and after (w2) biomineralization and the mass changes were recorded. To accurately calculate the weight change and assess the mineralized value, the drying step was conducted after the biomineralization process. The weight gain of scaffolds PCL was normalized to the initial weight of the sample. The formula used to normalize the data was defined as the weight gain divided by the initial weight, multiplied by 300, given that the initial weight is approximately 300 mg.

2.6. Morphological observations

The morphology and topography of the uncoated and coated nanofibers were examined with the use of a field-emission scanning electron microscope (FE-SEM, Hitachi SU-70, Japan). The aligned arrays were pressed against and transferred to the SEM stubs with two parallel adhesive tapes on their surfaces. The samples were coated with platinum before observation. The diameter and fibril alignment of the electrospun nanofibers were determined using image analysis software (ImagePro) and Hough transform analysis. The Hough transform is employed in this study to leverage the global characteristics of the SEM image of PCL nanofibers for direct detection of the target contour and subsequent connection of edge pixels to form a closed boundary region. The mineral coating formed on the nanofibers at different conditions was evaluated to determine the optimal parameters.

2.7. Determination of the elemental composition of the coating

The elemental composition of the mineral coating on the fibers was measured with the use of an energy-dispersive X-ray spectroscopy (EDX). The contents of calcium, phosphate, and magnesium in the coating were observed. The ratios of calcium to phosphate (Ca/P) and calcium to magnesium (Ca/Mg) were determined by comparing the percentage by weight of calcium to the percentage by weight of phosphate or magnesium in the samples.

2.8. Crystallographic structural determination and chemical composition analysis

XRD and FTIR analyses were performed to identify the crystallographic structure and chemical composition of the mineral apatite on the scaffolds in both 5 × SBFs. The nanofibrous scaffolds were immersed in solutions for 12, 24, and 36 h at an oscillation speed of 200 rpm. The scaffold fiber bundle was cut from the stainless steel ring and placed into DCM for continuous stirring until completely dissolved. The mixture was centrifuged for 15 min at 4000 rpm. The supernatant was removed, and the minerals were rinsed in fresh DCM and centrifuged again to remove DCM. The mineralized powder was dried in a fume hood for 2 d to evaporate the residual DCM.

Thin-film XRD spectra were obtained using a Rigaku D/max X-ray diffractometer with Cu Kα radiation (2500VB2+/PC, 40 kV, 200 mA). The scanning range was from 5 to 60° with a step size of 4° min^{-1}. For FTIR measurements, the scanning range was between 4000 and 600 cm^{-1}, the resolution was 4 cm^{-1}, and the average scanning times were 128.

2.9. Human embryonic palatal mesenchymal (HEPM) cell culture on scaffolds

Human embryonic palatal mesenchymal cells (HEPM, CRL-1772, ATCC) were selected for their potential for osteogenic differentiation. The cells were seeded on the unmineralized and mineralized nanofibrous scaffolds at a density of 4×10^4 cells cm^{-2} and cultured in AMEM media with 10 % fetal bovine serum (FBS) at 37 °C in the presence of 5 % CO_2 for the entire study. Scaffolds mineralized for 24 h at oscillation speeds of 150 and 200 rpm were chosen (referred to as HA/PCL-150 and HA/PCL-200). The attachment, extension, and proliferation of the cells within the structures were observed.

An Alamar Blue assay was performed to evaluate cell proliferation. Briefly, HEPM cells were cultured on scaffolds for 1, 3, 5, and 7 days, and cell proliferation was measured against the control at each set time point according to the production protocol. The percentage reduction of Alamar blue was normalized relative to that of the control.

The morphology of HEPM cells incubated on unmineralized and mineralized scaffolds was studied on the fifth day of cell culture. Briefly, the cells were fixed in 4 % paraformaldehyde and stained with phalloidin 555 (actin-red) and 4′,6-diamidino-2-phenylindole (DAPI, nucleus-blue). The attachment, alignment, and morphology of the cells on the scaffolds were assessed by confocal microscopy. Each group contained three samples, and multiple locations were observed.

2.10. Statistical analysis

Graphpad prism7.0 software was used in this study, and the measured data were expressed as means ± standard deviations. First, the normal distribution and homogeneity variance tests were conducted. T-tests were performed between the two sample groups. Three or more groups of samples were statistically analyzed by one-way analysis of variance (ANOVA). Tukey's test was used for comparison between groups. A value of $P < 0.05$ was considered statistically significant.

3. Results

3.1. Stability and pH change of 5 × SBF

The pH value of our body fluid is stable owing to the acid-base buffer systems, which are pivotal for mineralization and bone formation. Thus, we first tested the pH value change of the modified 5 × SBF system. Fig. 1 shows the changes in pH values of the traditional 5 × SBF and modified 5 × SBF throughout the process of biomineralization. The pH value of the traditional 5 × SBF continued to rise from its initial value of 6.4–8.0, and the solution rapidly became cloudy within 2 h. Within the set of 5 % CO_2, the pH of the modified 5 × SBF increased to 6.8, within 2 h, and then remained relatively stable. The solution remained clear throughout the biomineralization process and showed no signs of precipitation.

3.2. Weight gain of scaffolds

The aligned PCL nanofibers were developed and utilized as a model for further testing the mineralization ability of the modified SBF solution. The collected PCL nanofibers were uniform with an average diameter of 0.86 ± 0.20 μm, and the surfaces of the fibers were smooth (Fig. 2A–D). The Hough transform was used to analyze the alignment of the fibers, and the average angular deviation of the nanofibers was 7.1° (Fig. 2C). In the process of biomimetic mineralization, the weights of scaffolds in the traditional SBF solution increased slowly. However, after soaking them in the modified 5 × SBF, the weights of the scaffolds increased fast (Fig. 2E and F). This result indicates that the modified SBF solution could fasten the mineralization process.

3.3. Microstructure of mineral coating on scaffolds under modified SBF solutions

To further investigate the morphology of the microstructure of mineralized coatings, SEM images were captured during the mineralization process under traditional and modified SBF solutions at the oscillation speeds of 0,150, and 200 rpm (Figs. 3–5). Results showed that the microstructure of mineralized coatings or particles of all groups in the traditional 5 × SBF always maintained a homogeneous appearance during the entire biomineralization process (Fig. 3A). In the modified 5 × SBFs, the deposition behavior and morphology of the mineral apatite were different (Fig. 3B). In the initial 12 h, sparse mineralization centers first appeared on the surface of the fibers. The apatite centers gradually grew and merged into flakes as biomineralization progressed. After 36 h, the surface of the fibers was completely covered by an even apatite layer, and a lamellar heterogeneous structure was observed, which was remarkably different from those formed in the traditional 5 × SBFs (Fig. 3B). The movement and exchange of calcium and phosphorus ions in 5 × SBF were enhanced with increasing solution oscillation speed, thereby promoting the growth of apatite on the fiber surface. Thus, the biomineralization process occurred faster with an increase in the oscillation speed. When the oscillation velocities of the solution were 150 and 200 rpm, the time for the lamellar morphology to be observed was 24 h (Fig. 4A and B) and 12 h (Fig. 5A and B), respectively. A thick layer containing many agglomerations can be observed on the scaffolds at each set time at an oscillation speed of 200 rpm (Fig. 5A and B). Thus, in addition to accelerating biomineralization, the present study demonstrates that the incorporation of 5 % CO_2 into 5 × SBF significantly influences the microscopic morphology of the mineralized coating on the fiber surface. Compared to conventional 5 × SBF, modification with 5 % CO_2 in 5 × SBF induces a transformation of the mineralized coating from a homogeneous block-like structure to a heterogeneous porous and layered structure, resembling the natural bone structure observed in humans.

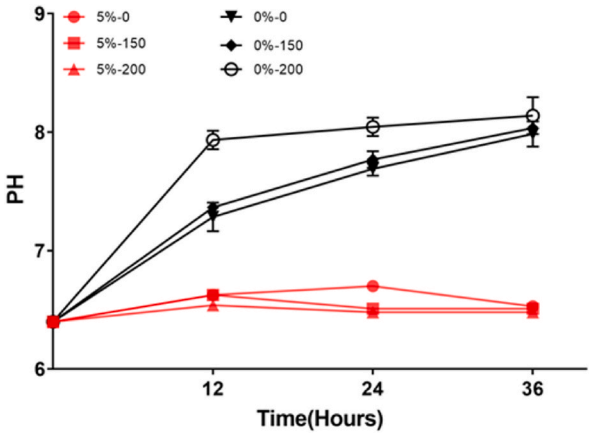

Fig. 1. Changes of pH values in traditional five times simulated body fluid (5 × SBF) and modified 5 × SBF with immersion time at the oscillation speeds of 0, 150, and 200 revolutions per minute (rpm).

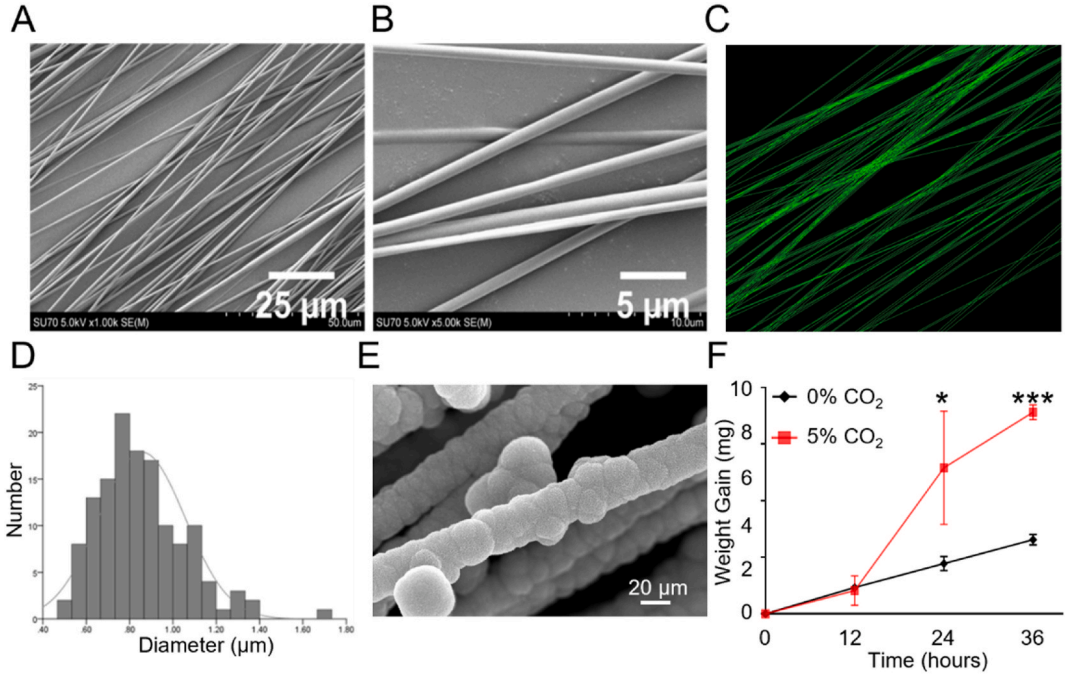

Fig. 2. Weight gain of aligned PCL nanofibers in modified SBF solution. (A, B) SEM of highly aligned nanofibrous scaffold. (C) The average angular deviation of the nanofibrils was 7.1°, as determined by Hoffman analysis. (D) The collected PCL nanofibers were uniform with an average diameter of 0.86 ± 0.20 μm. (E) SEM image depicting the morphology of mineralized crystallization under modified SBF solutions. (F) Weight increments of polycaprolactone (PCL) nanofibrous scaffolds with immersion time in the traditional and modified 5 × SBF solutions. The biomineralization experiment was conducted at an oscillation speed of 200 rpm.

3.4. Elemental composition and crystallographic structure of mineral coating on scaffolds under modified SBF solutions

The FTIR spectra of the apatites scratched from scaffolds immersed in both 5 × SBFs at an oscillation speed of 200 rpm for 24 h are shown (Fig. 6A and B). The absorption bands between 3500 cm^{-1} and 3000 cm^{-1} were attributed to H_2O. The band at PO_4^{3-} was shown by the presence of 1010 cm^{-1}. Peaks in the range of 1500–1385 cm^{-1} included the contributions of CO_3^{2-}. The band gradually widened with the increase in immersion time, thus indicating that the PO_4^{3-} moiety of apatite was partially and gradually replaced by CO_3^{2-}in apatite to form carbonated hydroxyapatite. XRD analysis further confirmed the presence of hydroxyapatite (HA). The XRD spectra of all minerality formed on the fibers incubated in both 5 × SBFs were similar, independent of the oscillation speed and immersion time. Only a broad peak was detected for 2θ angles in the range of 25–35°, thus indicating the formation of less crystallized or amorphous Ca–P phases (Fig. 6C and D). These results indicate that, compared with traditional SBF solution, the elemental composition of mineral coating was more similar to the biological hydroxyapatite in the natural bone under modified SBF solution. In addition, the elemental composition of mineral coating maintained unchanged under modified SBF solution. The EDX analysis of the PCL fibrous scaffolds after incubation in both SBFs are determined (Fig. 6E and F). In both 5 × SBFs, the Ca/P ratio of apatites formed on the fibers was lower than the theoretical stoichiometric Ca/P ratio of 1.67. However, with the increase in immersion time and oscillation speed, the mineral apatite formed in the modified 5 × SBF showed an increasing trend in the Ca/P ratio, especially after the formation of the flaky heterogeneous coating. Compared with the apatites formed in traditional 5 × SBF, the Ca/Mg ratio of mineral depositions formed in modified 5 × SBF was higher.

3.5. Biocompatibility evaluation of HA-PCL under modified SBF solution

The scaffolds were co-cultured with HEPM cells for seven days (Fig. 7A–C). The cytoskeleton and nuclei were stained and observed with the use of a confocal microscope. The HEPM cells adhered and proliferated on the PCL and HA/PCL scaffolds. The cell densities of the HA-PCL scaffolds under modified SBF solution were similar to those of the PCL scaffolds. The morphology of cells on the HA-PCL scaffolds under modified SBF solution was similar to that of the PCL fiber scaffolds, and the polarity distribution of the cytoskeleton was consistent with the fiber orientation. Quantification results of cell proliferation further confirmed these findings (Fig. 8A–D). The above results indicated that the uniform mineralized coating on the fiber surface showed good biocompatibility and have potential for inducing biomineralization under modified SBF solution.

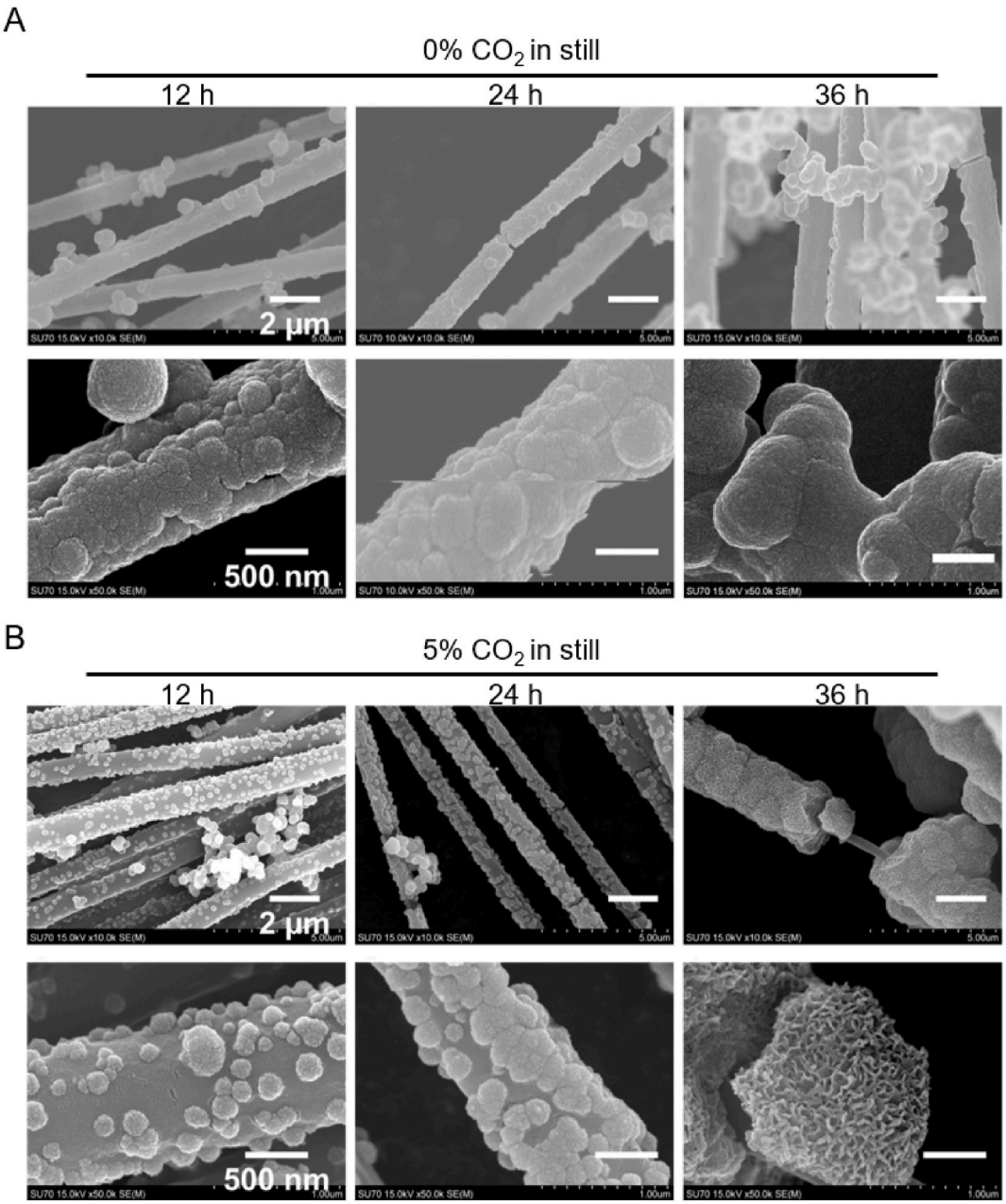

Fig. 3. Scanning electron microscopy (SEM) images depicting the morphology of mineralized crystallization under traditional and modified SBF solutions in still. (A) SEM images of PCL scaffolds soaked in still, traditional 5 × SBF for 12 h, 24 h, and 36 h at low (up panel, scale bar 2 μm) and high magnifications (down panel, scale bar 500 nm). (B) SEM images of PCL scaffolds soaked in still, modified 5 × SBF for 12 h, 24 h, and 36 h at low (up panel, scale bar 2 μm) and high magnifications (down panel, scale bar 500 nm).

4. Discussion

The simulation of the extracellular matrix (ECM) of natural bone is crucial in bone tissue engineering [23,24]. Generally, biomineralization with SBFs is considered to be a quick and convenient method for the mineralized coating of polymeric composites [25,26]. Supersaturated SBFs have been adopted by researchers to accelerate the biomineralization process. In addition to timesaving, supersaturated SBFs are particularly suitable for biomaterials with a rapid degradation rate [14,19]. However, homogeneous nucleation and deposition of calcium and phosphate minerals inevitably occurred in supersaturated SBFs owing to HCO_3^- decomposition and escape of gaseous CO_2 [14–16,19]. As the concentration of HCO_3^- in the solution increases, the rate of decomposition increases [17]. Our findings on the biomineralization of PCL nanofibrous scaffolds in traditional 5 × SBF were consistent with this view. The pH of the

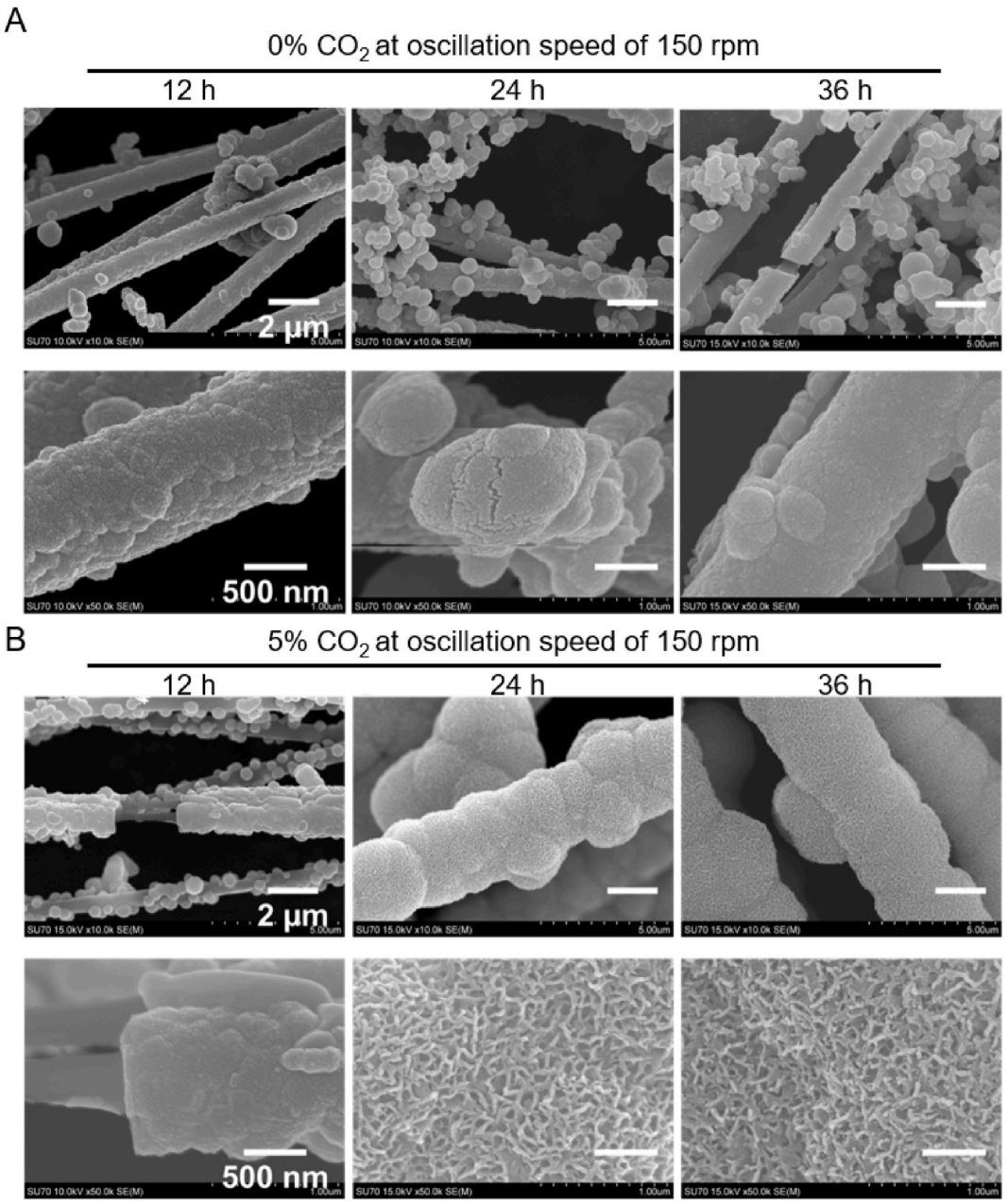

Fig. 4. Scanning electron microscopy (SEM) images depicting the morphology of mineralized crystallization under traditional and modified SBF solutions at oscillation speed of 150 rpm. (A) SEM images of PCL scaffolds soaked under traditional 5 × SBF for 12 h, 24 h, and 36 h at low (up panel, scale bar 2 μm) and high magnifications (down panel, scale bar 500 nm). (B) SEM images of PCL scaffolds soaked under modified 5 × SBF for 12 h, 24 h, and 36 h at low (up panel, scale bar 2 μm) and high magnifications (down panel, scale bar 500 nm).

traditional 5 × SBF continually increased up to 8.0, and the solution became turbid in 2 h owing to the occurrence of homogeneous precipitation of apatite crystals. In the SBF, the homogeneous precipitation of calcium salt and the nucleation and growth of calcium salt on fibers occurred simultaneously and competed with each other [15]. Therefore, the Ca–P formation on the fibers in the traditional 5 × SBF was postponed owing to the reduction of the ionic strengths of calcium and phosphorus caused by the significant precipitation of calcium salt at the initial stage of biomimetic mineralization. The large amount of loose spherical calcium salt particles on the fibers of group at the oscillation speeds 200 was prone to be the result of the precipitated calcium salt captured by the fibers at high-oscillation speeds, rather than the nucleation and growth of calcium salt on the fibers. In addition, the mineralized coating on the fiber surface maintained a lumpy and homogeneous appearance with a low Ca/P ratio throughout the entire biomimetic process in traditional 5 × SBF.

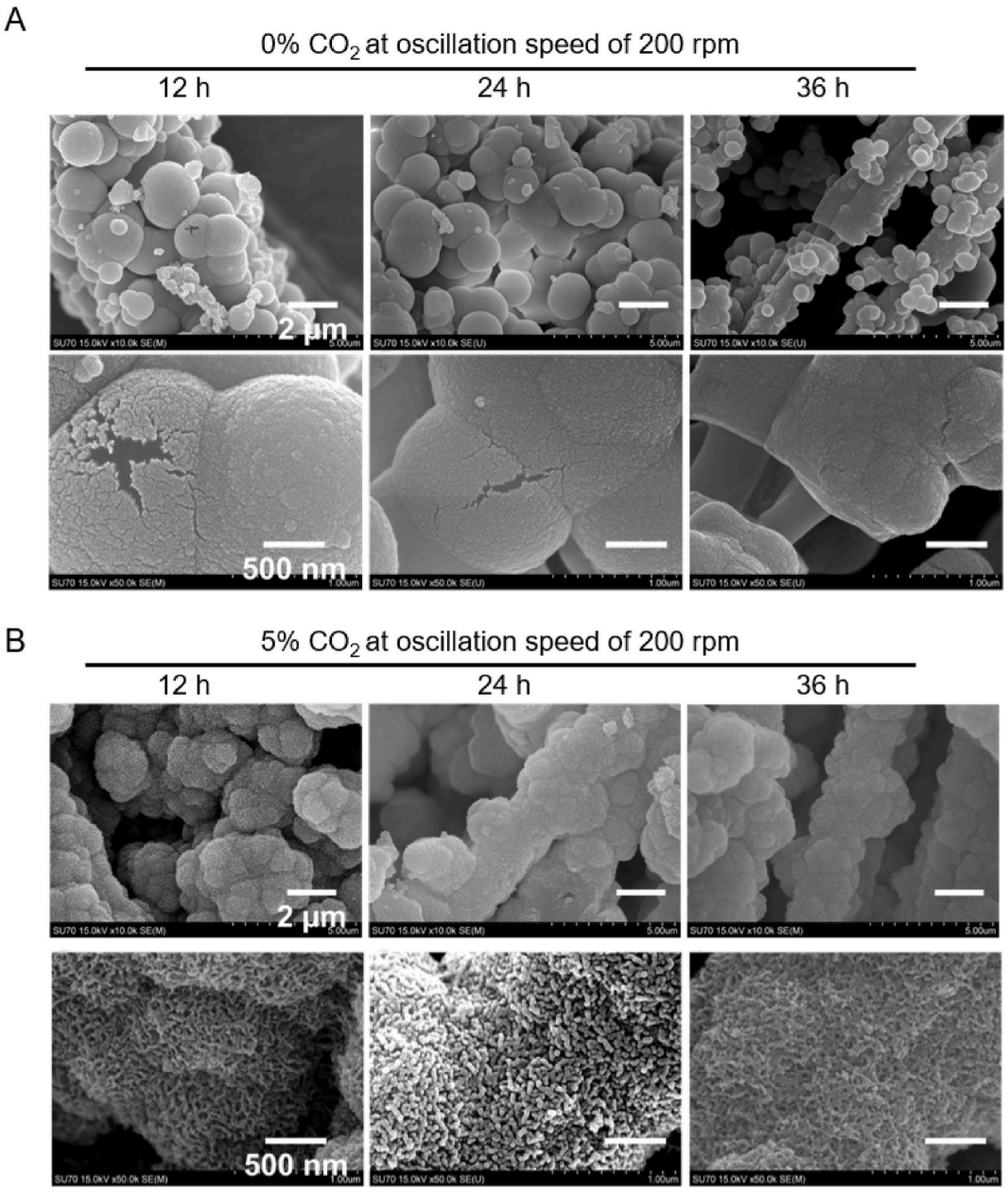

Fig. 5. Scanning electron microscopy (SEM) images depicting the morphology of mineralized crystallization under traditional and modified SBF solutions at oscillation speed of 200 rpm. (A) SEM images of PCL scaffolds soaked under traditional 5 × SBF for 12 h, 24 h, and 36 h at low (up panel, scale bar 2 μm) and high magnifications (down panel, scale bar 500 nm). (B) SEM images of PCL scaffolds soaked under modified 5 × SBF for 12 h, 24 h, and 36 h at low (up panel, scale bar 2 μm) and high magnifications (down panel, scale bar 500 nm).

In this study, a stable and highly efficient 5 × SBF in 5 % CO_2 was developed. The increase in pH values of traditional 5 × SBF and the formation of homogeneous apatite were attributed to the decomposition of HCO_3^- and the escape of gaseous CO_2. The solubility of CO_2 in water was approximately 23.6 mm at 37 °C, and the pKa of the formed H_2CO_3 which decomposed to HCO_3^- and H^+ was 6.35 [27]. These two data points are close to the initial concentration of HCO_3^- and the pH value of the traditional 5 × SBF. The continuous CO_2 gas supply helped overcome the decomposition equilibration reaction of HCO_3^-. The pH value of 5 × SBF in the presence of 5 % CO_2 remained stable at approximately 6.8, and the solution remained clear throughout the entire biomimetic process. Human blood was buffered mainly by a balance between carbonates and 5 % CO_2 in serum [28]. Therefore, it was more reasonable to perform biomineralization with the use of this type of modified 5 × SBF, which resembles human serum. In addition, in the modified 5 × SBF, the growth and deposition of apatite on nanofibrous scaffolds increased as a function of the dipping time. The rate of increase can be further modified by the oscillation speed. Shortening the immersion time is particularly important for biodegradable polymers, as

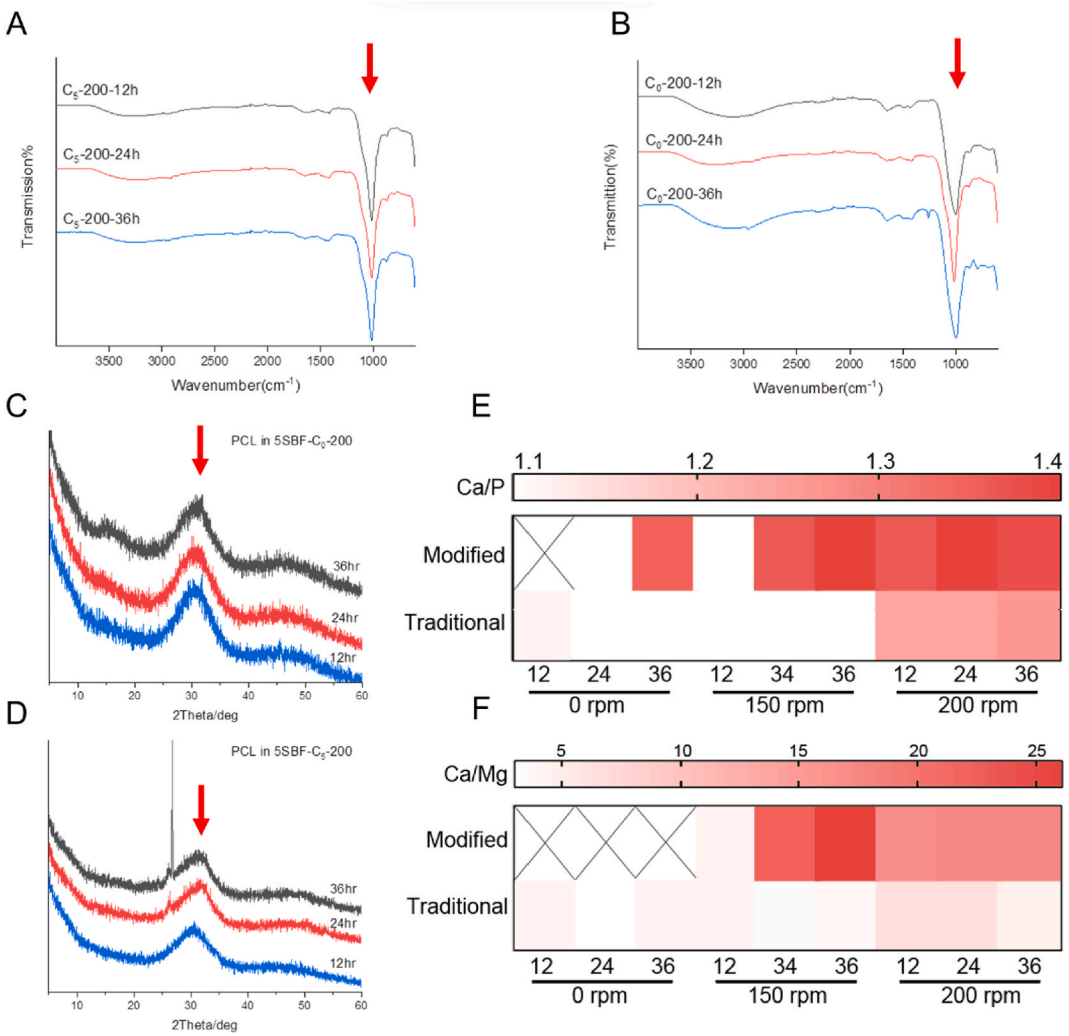

Fig. 6. Elemental composition and crystallographic structure of mineral coating on scaffolds under modified SBF solutions. (A, B) Changes of Fourier transform infrared (FTIR) spectra of PCL fibrous scaffolds with immersion time in the modified and traditional 5 × SBF solutions at an oscillation speed of 200 rpm. The red arrows indicate the peeks of PO_4^{3-}. (C, D) Changes of X-ray diffraction spectra of PCL fibrous scaffolds with immersion time in the modified and traditional 5 × SBF solutions at an oscillation speed of 200 rpm. The broad peaks indicated by the red arrow suggest that the crystal size of the coating is relatively small, implying the formation of amorphous mineralization and carbonated apatite. (E, F) Ca/P and Ca/Mg ratio of the apatites deposited on PCL scaffolds with soaking time in the traditional and modified 5 × SBF solutions at the oscillation speeds of 0,150, and 200 rpm.

some of them can degrade considerably during prolonged incubation periods.

The heterogeneous nucleation and growth process of apatite on the fiber surface in the modified 5 × SBF was observed based on SEM images. After hydrolysis with NaOH (0.1 N), the surface of PCL fibers was rich in hydroxyl and carboxyl functional groups [29]. Ca ions in the simulated body fluid could not be absorbed onto the PCL fiber surface and calcium phosphate formed via chemical bonds. Multiple crystal nuclei first appeared and grew with the increase in immersion time, and a uniform mineralized coating covered the entire surface of the fibers. In the modified 5 × SBF, the morphology of the mineralized coating was bound to transform to a heterogeneous lamellar structure. This transformation rate could be accelerated by the oscillation speed because of the increased exchange rate of ions in the solution. The combination of small crystals and the tiny space between them were closer to the microstructure of bone and resulted in a "yield zone," which provided toughness and strength [30].

Based on the atomic composition analysis, it was found that the apatite formed in the traditional 5 × SBF was poorly crystallized calcium-deficient hydroxyapatite, and the Ca/P ratios were as low as 1.1–1.2. However, a Ca/P ratio greater than 1.3 was achieved after the formation of a coating with a flaky microstructure in the modified 5 × SBF. This value was similar to the Ca/P ratio of biological hydroxyapatite in the natural bone. The ionic composition of human plasma was complex, and the HCO_3^- content was high. It is not difficult to imagine that HCO_3^- is also involved in bone growth and development. Recent hard tissue composition analysis has shown that there are CO_3^{2-}, Mg^{2+}, and Na^+ substitutions in bone tissue [31,32]. The FTIR and XRD results showed that the mineralized

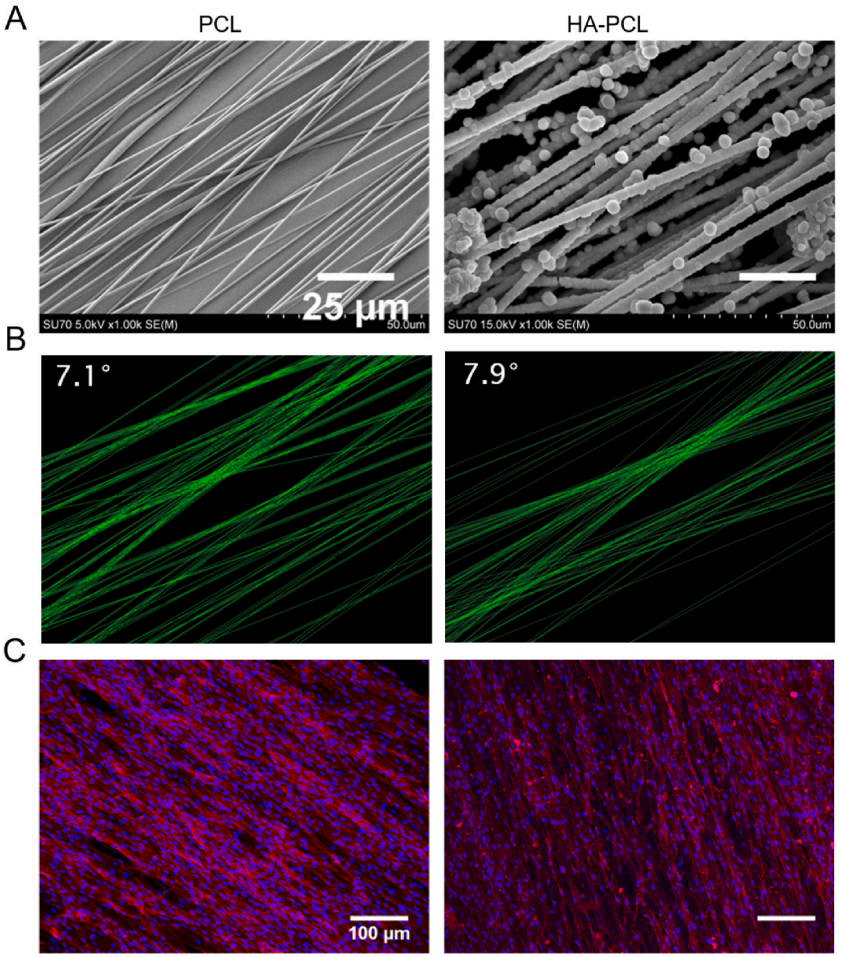

Fig. 7. Biocompatibility evaluation of HA-PCL under modified SBF solution. (A) SEM photographs of PCL fibrous scaffolds and scaffolds immersed in the modified 5 × SBF for 24 h. (B) Hough transform analysis of the fibers. (C) Immunohistochemical staining images of cells cocultured with scaffolds for 5 days.

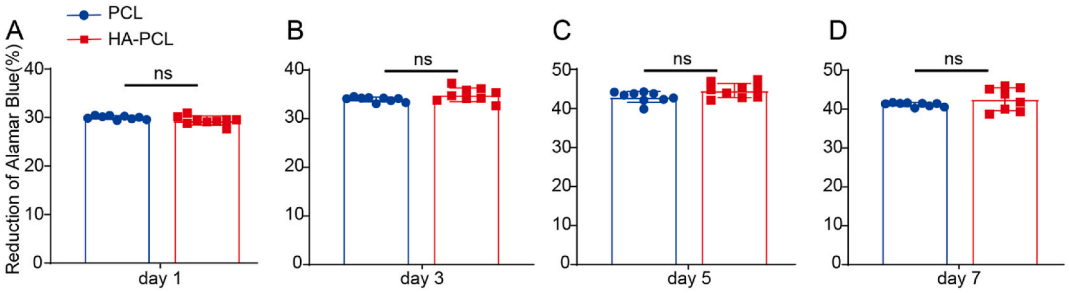

Fig. 8. Biocompatibility evaluation of HA-PCL under modified SBF solution. Human embryonic palatal mesenchymal (HEPM) cell proliferation on PCL and HA-PCL scaffolds at day 1 (A), day 3 (B), day 5 (C), and day 7 (D) (*$P < 0.05$, ***$P < 0.001$, ****$P < 0.0001$).

coating was characteristic of a less crystallized and carbonated Ca–P phase. In addition, with an increase in the oscillation speed of the solution, the movement and exchange of calcium phosphate ions in 5 × SBF are enhanced, thereby facilitating the growth of hydroxyapatite on the fiber surface. Thus, the oscillation speed is a critical factor in enhancing the surface mineralization of PCL fibers using 5 × SBF. Overall, the apatite formed on the surfaces of scaffold fibers in the 5 × SBF system in the presence of 5 % CO_2 was much more similar to bone apatite in structure and composition.

The present study determined the appropriate treatment methods and parameters for optimal mineralization of nanofibril scaffolds. These highly aligned biomineralized nanofibrous scaffolds were fabricated to closely mimic natural bone (in terms of structure and

composition) on which the osteoprogenitor cells demonstrated excellent attachment, alignment, and proliferation, thereby suggesting the attractiveness of these scaffolds for bone tissue engineering.

In addition, the simulated body fluid is typically considered useful for predicting the bioactivity of biomaterials in vitro. However, the rationality of using supersaturated SBFs, including 5 × SBF, to test bone-bonding bioactivity has been questioned [17,33]. This is because the precipitated homogeneous apatite crystals would attach to the surface of any biomaterial. A consensus has been reached such that the deposition of heterogeneous apatite on the surface of biomaterials is the primary requirement for bioactivity assessment with the use of SBF. In this study, the 5 × SBF in the presence of CO_2 partial pressure was stable, and a more important heterogeneous mineralized coating could be formed on biomaterials within a short time period. Therefore, this type of modified 5 × SBF could be used as a medium for predicting the bone-binding capacity of biomaterials in vivo. In addition, the entire biomineralization process, which was completed in a water-based medium in mild reaction conditions, is favorable for surface modification of three-dimensional porous biomaterials, and the simple operation of CO_2 partial pressure setting is conducive to the clinical application of this technology.

5. Conclusion

The modified 5 × SBF, in the presence of a 5 % CO_2 partial pressure, exhibits excellent stability and can be utilized for efficient heterogeneous biomineralization of polymer nanofibrous scaffolds without the need for additional buffer agents. Furthermore, by adjusting the immersion time and oscillation speed, the deposition of apatite can be further tailored. The biomimetic aligned nanofiber scaffold demonstrates remarkable biocompatibility. This entire biomineralization process is highly favorable for surface modification of three-dimensional porous biomaterials, while the simple operation of CO_2 partial pressure setting facilitates its clinical application. Moreover, utilizing the modified 5 × SBF enables accurate prediction of bone-bonding bioactivity in biomaterials and hydroxyapatite growth in solution. Additionally, it is necessary to further evaluate various types of bone tissue engineering materials in a modified SBF solution with a 5 % CO_2 concentration to assess the universality of 5 × SBF buffered by 5 % CO_2 in promoting material biomineralization. Furthermore, appropriate animal models should be employed for conducting in vivo assessment of the bone regenerative potential of the mineralized material in a modified simulated body fluid solution.

Data availability statement

All available data generated by experiments mentioned in this article are included in the manuscript. Raw datasets used and/or analyzed during the current study are available from the corresponding authors upon reasonable request.

CRediT authorship contribution statement

Kun Fu: Writing – review & editing, Validation, Supervision, Project administration, Investigation, Funding acquisition. **Lei-Lei Yang:** Writing – review & editing. **Ning Gao:** Validation, Funding acquisition. **Pengbi Liu:** Investigation. **Bo Xue:** Investigation. **Wei He:** Formal analysis, Supervision, Validation, Writing – review & editing. **Weiliu Qiu:** Formal analysis, Supervision, Validation, Writing – review & editing. **Xuejun Wen:** Supervision, Validation, Writing – review & editing, Conceptualization.

Declaration of competing interest

The authors declare that they have no known competing financial interests or personal relationships that could have appeared to influence the work reported in this paper.

Acknowledgements

This work was supported by the Medical Science and Technique Foundation of He'nan Province (No. SBGJ202102168), Foundation of He'nan Educational Committee (No. 22A320062), and Science and Technique Project of He'nan Province (No. 232102311025).

References

[1] G.L. Koons, M. Diba, A.G. Mikos, Materials design for bone-tissue engineering, Nat. Rev. Mater. 5 (2020) 584–603, https://doi.org/10.1038/s41578-020-0204-2.

[2] S. Wei, J.X. Ma, L. Xu, X.S. Gu, X.L. Ma, Biodegradable materials for bone defect repair, Mil Med Res 7 (2020) 54, https://doi.org/10.1186/s40779-020-00280-6.

[3] S. Tang, Z. Dong, X. Ke, J. Luo, J. Li, Advances in biomineralization-inspired materials for hard tissue repair, Int. J. Oral Sci. 13 (2021) 42, https://doi.org/10.1038/s41368-021-00147-z.

[4] R. Longo, M. Raimondo, L. Vertuccio, M.C. Ciardulli, M. Sirignano, A. Mariconda, G. Della Porta, L. Guadagno, Bottom-up strategy to forecast the drug location and release kinetics in antitumoral electrospun drug delivery systems, Int. J. Mol. Sci. 24 (2023), https://doi.org/10.3390/ijms24021507.

[5] V. Beachley, E. Katsanevakis, N. Zhang, X. Wen, A novel method to precisely assemble loose nanofiber structures for regenerative medicine applications, Adv Healthc Mater 2 (2013) 343–351, https://doi.org/10.1002/adhm.201200125.

[6] R.A. Ilyas, M.Y.M. Zuhri, M.N.F. Norrrahim, M.S.M. Misenan, M.A. Jenol, S.A. Samsudin, N.M. Nurazzi, M.R.M. Asyraf, A.B.M. Supian, S.P. Bangar, R. Nadlene, S. Sharma, A.A.B. Omran, Natural fiber-reinforced polycaprolactone green and hybrid biocomposites for various advanced applications, Polymers 14 (2022), https://doi.org/10.3390/polym14010182.

[7] Y. Gao, A. Callanan, Influence of surface topography on pcl electrospun scaffolds for liver tissue engineering, J. Mater. Chem. B 9 (2021) 8081–8093, https://doi.org/10.1039/d1tb00789k.

[8] A. Azari, A. Golchin, M. Mahmoodinia Maymand, F. Mansouri, A. Ardeshirylajimi, Electrospun polycaprolactone nanofibers: current research and applications in biomedical application, Adv. Pharmaceut. Bull. 12 (2022) 658–672, https://doi.org/10.34172/apb.2022.070.
[9] G. Onak, O. Karaman, Accelerated mineralization on nanofibers via non-thermal atmospheric plasma assisted glutamic acid templated peptide conjugation, Regen Biomater 6 (2019) 231–240, https://doi.org/10.1093/rb/rbz014.
[10] T. Kokubo, H. Takadama, How useful is sbf in predicting in vivo bone bioactivity? Biomaterials 27 (2006) 2907–2915, https://doi.org/10.1016/j.biomaterials.2006.01.017.
[11] T. Kokubo, S. Yamaguchi, Simulated body fluid and the novel bioactive materials derived from it, J. Biomed. Mater. Res. 107 (2019) 968–977, https://doi.org/10.1002/jbm.a.36620.
[12] D. Suarez-Gonzalez, K. Barnhart, F. Migneco, C. Flanagan, S.J. Hollister, W.L. Murphy, Controllable mineral coatings on pcl scaffolds as carriers for growth factor release, Biomaterials 33 (2012) 713–721, https://doi.org/10.1016/j.biomaterials.2011.09.095.
[13] L. Muller, F.A. Muller, Preparation of sbf with different hco3- content and its influence on the composition of biomimetic apatites, Acta Biomater. 2 (2006) 181–189, https://doi.org/10.1016/j.actbio.2005.11.001.
[14] D. Barati, J.D. Walters, S.R. Shariati, S. Moeinzadeh, E. Jabbari, Effect of organic acids on calcium phosphate nucleation and osteogenic differentiation of human mesenchymal stem cells on peptide functionalized nanofibers, Langmuir 31 (2015) 5130–5140, https://doi.org/10.1021/acs.langmuir.5b00615.
[15] F. Barrere, C.A. van Blitterswijk, K. de Groot, P. Layrolle, Influence of ionic strength and carbonate on the ca-p coating formation from sbfx5 solution, Biomaterials 23 (2002) 1921–1930, https://doi.org/10.1016/s0142-9612(01)00318-0.
[16] S. Chahal, S.J. Fathima, M.B. Yusoff, Biomimetic growth of bone-like apatite via simulated body fluid on hydroxyethyl cellulose/polyvinyl alcohol electrospun nanofibers, Bio Med. Mater. Eng. 24 (2014) 799–806, https://doi.org/10.3233/BME-130871.
[17] Q. Cai, Q. Xu, Q. Feng, X. Cao, X. Yang, X. Deng, Biomineralization of electrospun poly(l-lactic acid)/gelatin composite fibrous scaffold by using a supersaturated simulated body fluid with continuous co2 bubbling, Appl. Surf. Sci. 257 (2011) 10109–10118, https://doi.org/10.1016/j.apsusc.2011.06.157.
[18] L.M. Ingo Hofmann, Peter Greil, Frank A. Müller, Calcium phosphate nucleation on cellulose fabrics, Surf. Coating. Technol. 201 (2006) 2392–2398, https://doi.org/10.1016/j.surfcoat.2006.04.007.
[19] A.C. Jayasuriya, C. Shah, N.A. Ebraheim, A.H. Jayatissa, Acceleration of biomimetic mineralization to apply in bone regeneration, Biomed. Mater. 3 (2008) 015003, https://doi.org/10.1088/1748-6041/3/1/015003.
[20] F. Han, P. Zhang, T. Chen, C. Lin, X. Wen, P. Zhao, A lbl-assembled bioactive coating modified nanofibrous membrane for rapid tendon-bone healing in acl reconstruction, Int. J. Nanomed. 14 (2019) 9159–9172, https://doi.org/10.2147/IJN.S214359.
[21] Y. Chen, A. Mak, J. Li, M. Wang, A. Shum, Formation of apatite on poly(alpha-hydroxy acid) in an accelerated biomimetic process, J. Biomed. Mater. Res. B Appl. Biomater. 73 (2005) 68–76, https://doi.org/10.1002/jbm.b.30178.
[22] W.L. Murphy, D.J. Mooney, Bioinspired growth of crystalline carbonate apatite on biodegradable polymer substrata, J. Am. Chem. Soc. 124 (2002) 1910–1917, https://doi.org/10.1021/ja012433n.
[23] X. Lin, S. Patil, Y.G. Gao, A. Qian, The bone extracellular matrix in bone formation and regeneration, Front. Pharmacol. 11 (2020) 757, https://doi.org/10.3389/fphar.2020.00757.
[24] M. Baroncelli, B.C.J. van der Eerden, S. Chatterji, E. Rull Trinidad, Y.Y. Kan, M. Koedam, I.A.J. van Hengel, R. Alves, L.E. Fratila-Apachitei, J.A.A. Demmers, J. van de Peppel, J. van Leeuwen, Human osteoblast-derived extracellular matrix with high homology to bone proteome is osteopromotive, Tissue Eng Part A 24 (2018) 1377–1389, https://doi.org/10.1089/ten.TEA.2017.0448.
[25] T. Basargan, N. Erdol-Aydin, G. Nasun-Saygili, Hydroxyapatite-chitosan biocomposites synthesized in the simulated body fluid and their drug loading studies, J. Mater. Sci. Mater. Med. 28 (2017) 180.
[26] K.M. Tohamy, I.E. Soliman, M. Mabrouk, S. ElShebiney, H.H. Beherei, M.A. Aboelnasr, D.B. Das, Novel polysaccharide hybrid scaffold loaded with hydroxyapatite: Fabrication, bioactivity, and in vivo study, Mater Sci Eng C Mater Biol Appl 93 (2018) 1–11.
[27] Y.M. P Zhu, T. Yonezawa, Investigation of apatite deposition onto charged surfaces in aqueous solutions using a quartz-crystal microbalance, J. Am. Ceram. Soc. 86 (2003) 782–790.
[28] J.C. Atherton, Acid–base balance: Maintenance of plasma ph, Anaesth. Intensive Care Med. 7 (2006) 427–431.
[29] M. Samiei, M. Aghazadeh, E. Alizadeh, N. Aslaminabadi, S. Davaran, S. Shirazi, F. Ashrafi, R. Salehi, Osteogenic/odontogenic bioengineering with co-administration of simvastatin and hydroxyapatite on poly caprolactone based nanofibrous scaffold, Adv. Pharmaceut. Bull. 6 (2016) 353–365, https://doi.org/10.15171/apb.2016.047.
[30] H.S. Gupta, J. Seto, W. Wagermaier, P. Zaslansky, P. Boesecke, P. Fratzl, Cooperative deformation of mineral and collagen in bone at the nanoscale, Proc. Natl. Acad. Sci. U.S.A. 103 (2006) 17741–17746.
[31] R.Z. LeGeros, Properties of osteoconductive biomaterials: calcium phosphates, Clin. Orthop. Relat. Res. 395 (2002).
[32] C. Rey, C. Combes C Fau - Drouet, M.J. Drouet C Fau - Glimcher, M.J. Glimcher, Bone mineral: Update on chemical composition and structure, Osteoporos. Int. 20 (2009) 1013–1021.
[33] M. Bohner, J. Lemaitre, Can bioactivity be tested in vitro with sbf solution? Biomaterials 30 (2009) 2175–2179, https://doi.org/10.1016/j.biomaterials.2009.01.008.